



Published in final edited form as:

Lab Invest. 2013 June ; 93(6): 711–719. doi:10.1038/labinvest.2013.62.

The *Justy* mutant mouse strain produces a spontaneous murine model of salivary gland cancer with myoepithelial and basal cell differentiation

Andreas L. Simons^{1,2,5,*}, Ping Lu^{3,*}, Katherine N. Gibson-Corley¹, Robert A. Robinson^{1,5}, David K. Meyerholz¹, and John D. Colgan^{3,4,5}

¹Department of Pathology, The University of Iowa, Iowa City, IA 52242 USA

²Interdisciplinary Human Toxicology Program, The University of Iowa, Iowa City, IA 52242 USA

³Interdisciplinary Immunology Graduate Program, The University of Iowa, Iowa City, IA 52242 USA

⁴Department of Internal Medicine, The University of Iowa, Iowa City, IA 52242 USA

⁵Holden Comprehensive Cancer Center, The University of Iowa, Iowa City, IA 52242 USA

Abstract

We previously identified a novel mutant mouse strain on the C3HeB/FeJ background named *Justy*. This strain bears a recessive mutation in the *Gon4l* gene that greatly reduces expression of the encoded protein, a nuclear factor implicated in transcriptional regulation. Here, we report that *Justy* mutant mice aged 6 months or older spontaneously developed carcinomas with myoepithelial and basaloid differentiation in salivary glands with an incidence of ~25%. Tumors developed proximate to submandibular glands and to a lesser extent in the sublingual and parotid glands. Histologically, tumors often had central cavitory lesions filled with necrotic debris that was lined by tumor cells and had spindle and epithelioid cell differentiation with lesser basaloid to clear cell features. Tumor tissue often had variable evidence of a high mitotic rate, pleomorphism and invasion into adjacent salivary glands. Neoplastic cells had diffuse immunoreactivity for pancytokeratin (AE1/AE3) and p63. While CK5/6 immunostaining was seen in the much of the tumor cells, it was often lacking in pleomorphic areas. Tumor cells lacked immunoreactivity for *alpha*-smooth muscle actin, S100, c-Kit and glial fibrillary acid protein. Additionally, tumors had immunoreactivity for phosphorylated and total epidermal growth factor receptor (EGFR), suggesting that EGFR signaling may participate in growth regulation of these tumors. These findings indicate that the salivary gland carcinomas occur spontaneously in *Justy* mice and that these tumors may offer a valuable model for study of EGFR regulation. Combined, our data suggest that *Justy* mice warrant further investigation for use as a mouse model for human salivary gland neoplasia.

Users may view, print, copy, download and text and data- mine the content in such documents, for the purposes of academic research, subject always to the full Conditions of use: http://www.nature.com/authors/editorial_policies/license.html#terms

Corresponding author: John D. Colgan, PhD, Department of Internal Medicine, University of Iowa, 375 Newton Road, 3270 CBRB, Iowa City, IA 52242, P: 319-335-9561, F: 319-353-4728.

*Contributed equally

Salivary gland tumors are histologically one of the most heterogeneous group of tumors as compared to tumors in other areas of the body, which presents significant difficulties in both diagnosis and management (1). Although malignant salivary gland tumors are rare, representing approximately 3–5% of all head and neck cancers, these tumors can be difficult to treat and high-grade tumors are associated with a poor prognosis (2). Efforts to appropriately diagnose and treat salivary gland tumors have been hampered by limited knowledge of molecular biomarkers that can serve as indicators of salivary gland tumorigenesis (3). Additionally, there is a lack of mouse models for spontaneous salivary gland tumor development, which would be valuable for studying the pathogenesis and treatment of this disease.

The most well-known salivary gland tumor models are the transgenic PLAG1-overexpressing mouse model to study salivary gland pleomorphic adenoma (4), and the *Apc^{-/-}/Pten^{-/-}* models to study acinic cell carcinoma (5). In addition, salivary gland tumors were also identified in transgenic mice originally intended to provide models for studying mammary gland tumors (6–8). In these strains, the mouse mammary tumor virus (MMTV) promoter was used to preferentially express different oncogenes in mammary glands (6–8). Consequently, salivary gland tumors that appeared in these mice were not characterized in detail, since these tumors were not the original focus of the work undertaken. Therefore, there is a need to identify new murine models of salivary gland tumorigenesis that represent the human malignancies. Such models would accelerate progress in identifying diagnostic tools and novel treatments for human salivary gland tumors.

Here we present characterization of salivary gland tumors that arise in a mutant mouse strain named *Justy*. These mice carry a recessive point mutation in a phylogenetically conserved gene called *Gon4l*, which encodes a nuclear protein that appears to have key role in regulating gene expression in the context of developmental pathways (9–11). In *Justy* mice, expression of *Gon4l* protein is dramatically reduced, resulting in a profound arrest in B cell development. We found that 25% of *Justy* mice spontaneously develop salivary gland tumors, suggesting that loss of *Gon4l* expression may be involved in salivary gland tumorigenesis in mice. We also characterized the morphologic and immunomarker phenotype of these tumors, including the possible role of epidermal growth factor receptor (EGFR) signaling. Our findings suggest that the *Justy* mouse strain may provide a tractable model for longitudinal study of salivary gland tumorigenesis and for testing therapeutics that target salivary gland tumors.

MATERIALS AND METHODS

Mice

All procedures involving mice were approved by the Institutional Animal Care and Use Committee (IACUC) of the University of Iowa and conformed to guidelines established by the National Institutes of Health (NIH). Mice homozygous for the *Justy* mutation in *Gon4l* (referred to here as *Justy* mice) have been previously described (9, 12, 13). *Justy* mice were generated C3HeB/FeJ (C3H) genetic background and subjected to a standard breeding scheme to isolate the relevant mutation. Afterward, the mutant strain was maintained by intercrossing *Justy* mice. A cohort of 55 *Justy* mice comprised of individuals aged 6 months

or older was monitored up to 12 months of age for overt signs of disease. A cohort of 25 wild-type C3H mice was maintained in parallel as controls. Mice that developed cervical swelling or enlargement of the neck area were euthanized with CO₂ inhalation and subject to a complete necropsy.

Tissues

At necropsy, cervical masses in affected mice were excised en bloc with adjacent salivary glands and immersion fixed in 10% neutral buffered formalin. Following fixation (approximately 5 days) tissues were routinely processed, paraffin-embedded, sectioned at 4 μm and stained with hematoxylin and eosin (HE). Markers of epithelial and mesenchymal tumor differentiation were assessed by immunohistochemistry (Table 1). The scoring for the immunohistochemical staining was as follows: “Neg” - none; “+” rare to 33% of tumor cells; “++” ~34% to 66% of tumor cells; “+++” ~67% to diffuse cellular immunostaining.

RESULTS

Gross Pathology

Individuals in a cohort of *Justy* mice aged 6 months and older were found to sporadically develop ventrolateral cervical masses (Figure 1) with an incidence of 25%. These masses were generally circumscribed, fluctuant to touch and when punctured would leak fluid contents that partially collapsed the tumor. The tumor tissue was often adherent to the adjacent salivary gland chain. Therefore, the tumor and salivary glands were prosected en bloc for fixation and study. Among the *Justy* mice, there was no bias in tumor development with respect to sex and no tumors were observed in a similarly aged cohort of wild-type C3H mice.

Histopathology

The solid tumors often had central, cavitory (pseudocystic) lesions (Figure 2A) and were intimately associated with salivary glands, compressing and invading the adjacent salivary glands (Figure 2 B, C). The cavitory lesions were filled by cellular debris and foamy macrophages, and lined by solid tumor tissue (Figure 3 A, B). The tumors were consistently associated with the submandibular salivary gland and to a lesser extent with the sublingual and parotid glands (Table 2). HE staining showed that tumors frequently contained a mixture of spindle cells interspersed with epitheloid cells and lesser basaloid to clear cell differentiation (Figure 3 C–F, Table 2). Pleomorphic foci characterized by anisokaryosis and anisocytosis with a high mitotic rate up to 5–10 mitoses/high power 60x objective (Figure 3B, inset) were variably detected in all tumors.

Immunohistochemical Staining

Tumors and adjacent salivary gland tissues from 5 mice were stained with a variety of immunohistochemical markers, and the results obtained are summarized in Table 3. AE1/AE3 (pancytokeratin) and p63 markers showed intense and widespread immunoreactivity in tumor cells (Figure 4 A, B). Similarly, cytokeratin 5/6 marker was immunoreactive in the majority of tumor cells (>50%) but was negative in foci that were pleomorphic (Figure 4C). *Alpha*-smooth muscle actin (SMA) was not detected in tumor cells

(Figure 4D). Most of the tumor cells also showed immunostaining for EGFR and phosphorylated EGFR (pEGFR), although immunostaining in the pEGFR sections was less extensive (Figure 4 E, F). Tumor cells lacked GFAP immunostaining except for rare solitary cells and were consistently negative for S100 and c-Kit immunoreactivity (Table 3). In normal submandibular salivary glands, *alpha*-SMA immunostaining was present in myoepithelial cells surrounding the epithelium of granular convoluted ducts, vessels and gland acini, but was absent in excretory ducts (Figure 5A). Additionally, p63 immunostaining was commonly seen subjacent to the excretory duct epithelium, but rarely detected around smaller convoluted ducts (Figure 5B).

DISCUSSION

The *Justy* strain was originally created and discovered by subjecting male mice to chemical mutagenesis and then screening offspring for abnormalities in peripheral blood cell populations (12, 13). Subsequent molecular analysis demonstrated that *Justy* mice carry a recessive point mutation within the *Gon4l* gene that disrupts splicing and thus the coding sequence of *Gon4l* mRNA, resulting in dramatically decreased levels of *Gon4l* protein in lymphoid cells (9). Moreover, in mice that are homozygous for the *Justy* mutation, B lymphopoiesis is abrogated, while other aspects of mouse hematopoiesis and physiology appear unaffected (9). These data demonstrate that the *Gon*-like has a critical role in B lineage cells. The results we report here strongly suggest that decreased expression of *Gon4*-like protein facilitates spontaneous salivary gland tumorigenesis. Thus, a worthwhile goal for future studies is to determine the role of *Gon4*-like in salivary gland development and function, which could ultimately identify pathways that are critical in the normal tissue and may be subverted in salivary gland neoplasia.

The molecular function of *Gon4l* is currently not well understood. However, as demonstrated in our previous studies, decreased *Gon4l* protein levels are associated with sustained expression of “non-B” genes that can antagonize B cell development and are normally downregulated at the transcriptional level during the early stages of B lymphopoiesis (9, 14). These findings suggest that *Gon4l* may have a key role in mechanisms that enforce gene repression in developing B cells. In support of this idea, studies in *Caenorhabditis elegans*, *Drosophila melanogaster* and zebrafish have all provided evidence that *Gon4l* is important for the regulation of gene expression in developmental pathways (10, 11, 15). We also found that the 250 kDa *Gon4l* protein forms complexes with the co-repressor molecule Sin3a and histone deacetylase 1 (HDAC1) (14). Complexes containing Sin3a and HDAC1 are usually involved in gene repression, and abnormal recruitment or activity of these complexes has been implicated in neoplastic transformation (16–20). For example, SMAD4 (MAD homologue 4) recruits and interacts with HDAC1 and Sin3a to form a complex involved in gene repression (21). Additionally, loss of SMAD4 in T cells leads to spontaneous epithelial tumors in the oral cavity and throughout the gastrointestinal tract (22, 23). These observations suggest that dysregulation of gene expression due to decreased levels of *Gon4*-like protein may be a key factor in the initiation of salivary gland tumorigenesis as it occurs in *Justy* mice.

Although we believe that loss of Gon4l expression is responsible for salivary gland tumor development in our studies, there remains a possibility that the lack of peripheral B cells in *Justy* mice is a factor that contributes to tumor development. However, we have found no evidence (using a literature search) of a high incidence of salivary gland tumors in B cell-deficient mice or in C3H mice. In fact, spontaneous salivary gland tumors are quite rare in mice, with the highest incidence of 4% being observed in the BALB/C strain (24, 25). We observed that *Justy* mice aged 6 months and older developed salivary gland tumors at an incidence of 25%, a rate well above that reported as background incidence for any inbred mouse strain. To our knowledge, an association between congenital B cell deficiencies in humans and increased incidence of salivary gland tumors has not been established, again suggesting that a lack B cells is not a dominant factor for this particular tumor type.

Based on the cellular pleomorphism, high mitotic rate and their invasive nature, the tumors in *Justy* mice were diagnosed as carcinomas (Figure 2B, C). The morphology of the tumors suggested myoepithelial origin due to the common presence of spindled and epitheloid differentiation (Figure 3C–F). Myoepithelial differentiation would be expected to have both cytokeratins and *alpha*-SMA immunostaining (26–28). However, while salivary gland tumor cells possessed immunoreactivity for cytokeratin and p63, the tumor cells lacked immunostaining for the *alpha*-SMA marker. The progenitor cell marker p63 is often expressed in basal cells as well as myoepithelial cells (26–28). Myoepithelial cells circumferentially line the epithelium of normal salivary gland acini and this relationship continues into the intralobular ducts. In contrast, excretory ducts lack myoepithelial cells but are preferentially lined by basal cells that can exhibit myoepithelial cell morphology (27) (Figure 5 A, B). Given the myoepithelial differentiation found in these tumors as well as the consistent *alpha*-SMA negative and p63 positive immunophenotype, these tumors would be consistent with a basal cell adenocarcinoma diagnosis having a likely origin from basal cells associated with excretory ducts.

The *Justy*-associated tumors did not have any resemblance to salivary duct carcinoma given the lack of intraductal or precursor lesions in the glandular tissue surrounding the tumors. Salivary duct carcinoma is a high grade malignancy and strongly resembles human mammary carcinoma, consisting of intraductal and invasive components and cribriform patterns in both components. The observed tumors did not show marked nuclear atypia as is uniformly seen in salivary duct carcinoma, nor did they have a cribriform growth pattern. Furthermore HER-2-Neu staining, which is typical of salivary duct carcinoma (29), was absent in these tumors (data not shown) again suggesting that these tumors were not salivary duct carcinomas.

The salivary gland neoplasms that develop in *Justy* mice mimic many of the findings seen in a subset of human basal cell adenocarcinoma with myoepithelial differentiation (30). This similarity to their human counterparts is manifest at multiple levels, including gross pathology, histologic morphology and antigen expression. The distinct peripheral palisading of basaloid cells present at the periphery of the tumor cell nests in *Justy* mice (Figure 3D) is highly reminiscent of basal cell adenocarcinomas in humans. These tumor cells exhibit the same immunohistochemical marker expression as human salivary gland tumors composed of basal cells. In addition to the basal cell differentiation, the spindled cell morphology present

in the *Justy* tumors (Figure 3C) appears identical in both character and amount to that seen in myoepithelial carcinomas occurring in human salivary glands. Furthermore, the tumor cells comprising these spindled areas stained strongly with p63 (Figure 4B), giving further support for basal cell adenocarcinoma with myoepithelial differentiation.

Certain antigens associated with human basal cell adenocarcinoma including S-100 and *alpha*-SMA, were not detected in our immunohistochemical analyses of tumors from *Justy* mice, (Table 3). However, while these antigens are often expressed in these neoplasms in humans, the literature documents that myoepithelial markers can be inconsistently expressed in these neoplasms (28, 31–33). *Justy*-associated tumors show areas of high histologic grade and are associated with a high mitotic rate and necrosis (Figure 3B), characteristic of those seen in basal cell adenocarcinomas and myoepithelial carcinomas. As another correlate to human tumors, the gross findings of the *Justy* tumors (Figure 1) are strikingly similar to myoepithelial carcinoma of the human salivary gland. Human myoepithelial carcinomas commonly show a multinodular growth pattern with cyst formation, which on histologic examination is seen to be pseudocyst formation (34). All of these features are identical to those displayed by salivary gland tumors from *Justy* mice.

Tumor cells from *Justy* mice were immunoreactive for EGFR and pEGFR (Table 3). Expression of EGFR has been investigated as a prognosis factor in several human salivary gland tumor studies (35–38). EGFR is important for cell growth, survival and differentiation (39–41) and enhanced activity or overexpression is associated with tumor progression and metastasis in many epithelial tumors, especially in head and neck tumors (42–44). Interestingly, EGFR is expressed in basal cell adenocarcinomas and its expression can be used to distinguish basal cell adenomas from basal cell adenocarcinomas (32). Finally, several types of salivary gland tumors overexpress EGFR, and EGFR inhibitors are of interest to treat these tumors [28–31]. The presence of pEGFR and EGFR expression in the tumors from *Justy* mice suggests that this model may be useful for studying the efficacy of EGFR inhibitors as a treatment for various forms of salivary gland cancer.

Limitations for the use of *Justy* mice as a salivary gland cancer mouse model are the relatively low penetrance of tumor formation and a long latency period compared to the well-known transgenic PLAG1 and *Apc*^{-/-}/*Pten*^{-/-} mouse models for salivary gland tumorigenesis (4, 5). However, the requirement for *Justy* mice to age before tumor onset along with the unilateral distribution actually parallels the clinical spectrum in humans, as salivary gland tumors are often unilateral and develop in the 5–6th decades of life (45, 46). Additionally, this study has revealed a novel association between Gon4l expression and mouse salivary gland tumorigenesis, which warrants further study.

Here we present a novel and feasible mouse model of salivary gland cancer that, with further investigation, may be used to study the consecutive steps involved in initiation and progression of salivary gland tumors. Existing salivary gland tumor models develop low grade (5) or benign tumors (4). However, in this mouse model the loss of Gon4l expression leads to the spontaneous development of intermediate grade salivary gland tumors that resemble basal cell adenocarcinoma, suggesting that impairment of Gon4l function or expression can initiate salivary gland tumorigenesis. At this time, it is unclear if Gon4l loss

is involved in human salivary gland neoplasia; this is currently being investigated. Additionally, improvements with respect to decreased latency period and increased penetrance need to be made in order for the *Justy* mouse to be used as a salivary gland tumor mouse model. Nevertheless, our study has revealed a previously unrecognized connection between *Gon4l* expression and salivary gland tumorigenesis, which may lead to new information about genes and pathways involved in human salivary gland cancer.

Supplementary Material

Refer to Web version on PubMed Central for supplementary material.

Acknowledgments

We thank the Comparative Pathology and Histology Research Laboratories in the Department of Pathology at the University of Iowa for technical assistance. This work is supported in part by NIH grant R01AI093737(JDC) as well as the Departments of Pathology and Internal Medicine at The University of Iowa.

References

1. Spiro RH. Salivary neoplasms: overview of a 35-year experience with 2,807 patients. *Head Neck Surg.* 1986; 8(3):177–184. [PubMed: 3744850]
2. Witt RL. Major salivary gland cancer. *Surg Oncol Clin N Am.* 2004; 13(1):113–127. [PubMed: 15062365]
3. Surakanti SG, Agulnik M. Salivary gland malignancies: the role for chemotherapy and molecular targeted agents. *Semin Oncol.* 2008; 35(3):309–319. [PubMed: 18544445]
4. Declercq J, Van Dyck F, Braem CV, et al. Salivary gland tumors in transgenic mice with targeted *PLAG1* proto-oncogene overexpression. *Cancer Res.* 2005; 65(11):4544–4553. [PubMed: 15930271]
5. Diegel CR, Cho KR, El-Naggar AK, et al. Mammalian target of rapamycin-dependent acinar cell neoplasia after inactivation of *Apc* and *Pten* in the mouse salivary gland: implications for human acinic cell carcinoma. *Cancer Res.* 2010; 70(22):9143–9152. [PubMed: 21062985]
6. Tsukamoto AS, Grosschedl R, Guzman RC, et al. Expression of the *int-1* gene in transgenic mice is associated with mammary gland hyperplasia and adenocarcinomas in male and female mice. *Cell.* 1988; 55(4):619–625. [PubMed: 3180222]
7. Lucchini F, Sacco MG, Hu N, et al. Early and multifocal tumors in breast, salivary, harderian and epididymal tissues developed in MMTV-*Neu* transgenic mice. *Cancer Lett.* 1992; 64(3):203–209. [PubMed: 1322235]
8. Taneja P, Frazier DP, Kendig RD, et al. MMTV mouse models and the diagnostic values of MMTV-like sequences in human breast cancer. *Expert Rev Mol Diagn.* 2009; 9(5):423–440. [PubMed: 19580428]
9. Lu P, Hankel IL, Knisz J, et al. The *Justy* mutation identifies *Gon4*-like as a gene that is essential for B lymphopoiesis. *J Exp Med.* 2010; 207(7):1359–1367. [PubMed: 20530203]
10. Friedman L, Santa Anna-Arriola S, Hodgkin J, et al. *gon-4*, a cell lineage regulator required for gonadogenesis in *Caenorhabditis elegans*. *Dev Biol.* 2000; 228(2):350–362. [PubMed: 11112335]
11. Liu Y, Du L, Osato M, et al. The zebrafish *udu* gene encodes a novel nuclear factor and is essential for primitive erythroid cell development. *Blood.* 2007; 110(1):99–106. [PubMed: 17369489]
12. Hrabe de Angelis MH, Flaswinkel H, Fuchs H, et al. Genome-wide, large-scale production of mutant mice by ENU mutagenesis. *Nat Genet.* 2000; 25(4):444–447. [PubMed: 10932192]
13. Augustin M, Sedlmeier R, Peters T, et al. Efficient and fast targeted production of murine models based on ENU mutagenesis. *Mamm Genome.* 2005; 16(6):405–413. [PubMed: 16075367]

14. Lu P, Hankel IL, Hostager BS, et al. The developmental regulator protein Gon4l associates with protein YY1, co-repressor Sin3a, and histone deacetylase 1 and mediates transcriptional repression. *J Biol Chem.* 2011; 286(20):18311–18319. [PubMed: 21454521]
15. Kitsiou-Tzeli S, Kolialexi A, Fryssira H, et al. Detection of 22q11.2 deletion among 139 patients with Di George/Velocardiofacial syndrome features. *In Vivo.* 2004; 18(5):603–608. [PubMed: 15523900]
16. Bansal N, Kadamb R, Mittal S, et al. Tumor suppressor protein p53 recruits human Sin3B/HDAC1 complex for down-regulation of its target promoters in response to genotoxic stress. *PLoS One.* 2011; 6(10):e26156. [PubMed: 22028823]
17. Liao M, Zhang Y, Dufau ML. Protein kinase Calpha-induced derepression of the human luteinizing hormone receptor gene transcription through ERK-mediated release of HDAC1/Sin3A repressor complex from Sp1 sites. *Mol Endocrinol.* 2008; 22(6):1449–1463. [PubMed: 18372343]
18. Sheeba CJ, Palmeirim I, Andrade RP. Chick Hairy1 protein interacts with Sap18, a component of the Sin3/HDAC transcriptional repressor complex. *BMC Dev Biol.* 2007; 7:83. [PubMed: 17623094]
19. Clem BF, Clark BJ. Association of the mSin3A-histone deacetylase 1/2 corepressor complex with the mouse steroidogenic acute regulatory protein gene. *Mol Endocrinol.* 2006; 20(1):100–113. [PubMed: 16109738]
20. Peinado H, Ballestar E, Esteller M, et al. Snail mediates E-cadherin repression by the recruitment of the Sin3A/histone deacetylase 1 (HDAC1)/HDAC2 complex. *Mol Cell Biol.* 2004; 24(1):306–319. [PubMed: 14673164]
21. Kim DW, Lassar AB. Smad-dependent recruitment of a histone deacetylase/Sin3A complex modulates the bone morphogenetic protein-dependent transcriptional repressor activity of Nkx3.2. *Mol Cell Biol.* 2003; 23(23):8704–8717. [PubMed: 14612411]
22. Hahn JN, Falck VG, Jirik FR. Smad4 deficiency in T cells leads to the Th17-associated development of premalignant gastroduodenal lesions in mice. *J Clin Invest.* 2011; 121(10):4030–4042. [PubMed: 21881210]
23. Kim BG, Li C, Qiao W, et al. Smad4 signalling in T cells is required for suppression of gastrointestinal cancer. *Nature.* 2006; 441(7096):1015–1019. [PubMed: 16791201]
24. Law LW, Dunn TB, Boyle PJ. Neoplasms in the C3H strain and in F1 hybrid mice of two crosses following introduction of extracts and filtrates of leukemic tissues. *J Natl Cancer Inst.* 1955; 16(2):495–539. [PubMed: 13263918]
25. Sundberg JP, Hanson CA, Roop DR, et al. Myoepitheliomas in inbred laboratory mice. *Vet Pathol.* 1991; 28(4):313–323. [PubMed: 1719689]
26. Batsakis JG, Regezi JA, Luna MA, et al. Histogenesis of salivary gland neoplasms: a postulate with prognostic implications. *J Laryngol Otol.* 1989; 103(10):939–944. [PubMed: 2685148]
27. Riva A, Serra GP, Proto E, et al. The myoepithelial and basal cells of ducts of human major salivary glands: a SEM study. *Arch Histol Cytol.* 1992; 55 (Suppl):115–124. [PubMed: 1290659]
28. Savera AT, Sloman A, Huvos AG, Klimstra DS. Myoepithelial carcinoma of the salivary glands: a clinicopathologic study of 25 patients. *Am J Surg Pathol.* 2000; 24(6):761–774. [PubMed: 10843278]
29. Clauditz TS, Reiff M, Gravert L, et al. Human epidermal growth factor receptor 2 (HER2) in salivary gland carcinomas. *Pathology.* 2011; 43(5):459–464. [PubMed: 21670724]
30. Robinson, RA. Salivary Gland. *Head and Neck Pathology-Atlas for Histologic and Cytologic Diagnosis.* Philadelphia: Lippincott Williams & Wilkins; 2010. p. 228-232.
31. Ellis, GL.; Auclair, P. Tumors of the Salivary Gland. *AFIP Atlas of Tumor Pathology.* Silver Spring: ARP Press; 2008. p. 347-348.
32. Nagao T, Sugano I, Ishida Y, et al. Basal cell adenocarcinoma of the salivary glands: comparison with basal cell adenoma through assessment of cell proliferation, apoptosis, and expression of p53 and bcl-2. *Cancer.* 1998; 82(3):439–447. [PubMed: 9452259]
33. Zheng S, Guo Y, Mones JM. Basal cell carcinoma with myoepithelial differentiation. *Am J Dermatopathol.* 2011; 33(8):863–866. [PubMed: 21885942]

34. Skalova, A.; Jakel, KT. Myoepithelial carcinoma. In: Barnes, L.; Eveson, JW.; Reichert, P.; Sidransky, D., editors. World Health Organization Classification of Tumours: Pathology & Genetics of Head and Neck Tumours. Lyon: IARC Press; 2005. p. 240
35. Ettl T, Baader K, Stiegler C, et al. Loss of PTEN is associated with elevated EGFR and HER2 expression and worse prognosis in salivary gland cancer. *Br J Cancer*. 2012; 106(4):719–726. [PubMed: 22240798]
36. Ettl T, Stiegler C, Zeitler K, et al. EGFR, HER2, survivin, and loss of pSTAT3 characterize high-grade malignancy in salivary gland cancer with impact on prognosis. *Hum Pathol*. 2012; 43(6): 921–931. [PubMed: 22154363]
37. Ettl T, Schwarz S, Kleinsasser N, et al. Overexpression of EGFR and absence of C-KIT expression correlate with poor prognosis in salivary gland carcinomas. *Histopathology*. 2008; 53(5):567–577. [PubMed: 18983466]
38. Monteiro LS, Bento MJ, Palmeira C, et al. Epidermal growth factor receptor immunoeexpression evaluation in malignant salivary gland tumours. *J Oral Pathol Med*. 2009; 38(6):508–513. [PubMed: 19317849]
39. Knox SM, Lombaert IM, Reed XV, et al. Parasympathetic innervation maintains epithelial progenitor cells during salivary organogenesis. *Science*. 2010; 329(5999):1645–1647. [PubMed: 20929848]
40. Prenzel N, Fischer OM, Streit S, et al. The epidermal growth factor receptor family as a central element for cellular signal transduction and diversification. *Endocr Relat Cancer*. 2001; 8(1):11–31. [PubMed: 11350724]
41. Zwick E, Hackel PO, Prenzel N, et al. The EGF receptor as central transducer of heterologous signalling systems. *Trends Pharmacol Sci*. 1999; 20(10):408–412. [PubMed: 10577253]
42. Rocha-Lima CM, Soares HP, Raez LE, et al. EGFR targeting of solid tumors. *Cancer Control*. 2007; 14(3):295–304. [PubMed: 17615536]
43. Ang KK, Berkey BA, Tu X, et al. Impact of epidermal growth factor receptor expression on survival and pattern of relapse in patients with advanced head and neck carcinoma. *Cancer Res*. 2002; 62(24):7350–7356. [PubMed: 12499279]
44. Grandis JR, Tweardy DJ. Elevated levels of transforming growth factor alpha and epidermal growth factor receptor messenger RNA are early markers of carcinogenesis in head and neck cancer. *Cancer Res*. 1993; 53(15):3579–3584. [PubMed: 8339264]
45. Eveson, JW.; Auclair, P.; Gnepp, DR., et al. Tumours of the salivary glands: Introduction. In: Barnes, L.; Eveson, JW.; Reichert, P.; Sidransky, D., editors. World Health Organization Classification of Tumours: Pathology & Genetics of Head and Neck Tumours. Lyon: IARC Press; 2005. p. 213
46. Ungari C, Paparo F, Colangeli W, et al. Parotid glands tumours: overview of a 10-year experience with 282 patients, focusing on 231 benign epithelial neoplasms. *Eur Rev Med Pharmacol Sci*. 2008; 12(5):321–325. [PubMed: 19024217]



Figure 1. Gross anatomy of salivary gland tumor in a *Justy* mouse
The overlying skin of the ventral cervical region was reflected to demonstrate a unilateral tumor, bar = 1.5 cm.

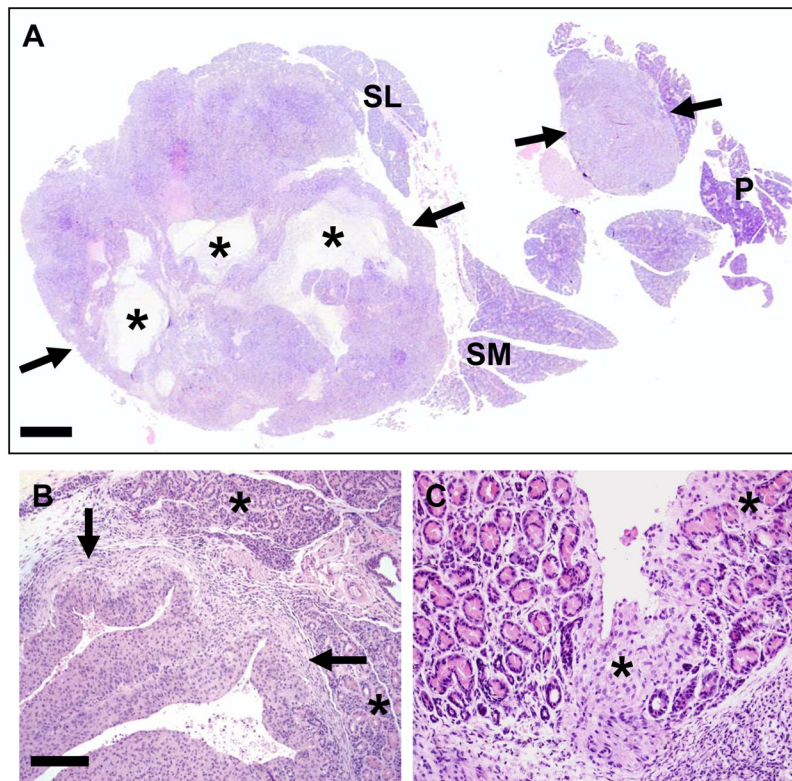


Figure 2. Salivary gland tumors in a *Justy* mouse

A) Sublingual (SL), submandibular (SM) and parotid (P) salivary glands. The tumors (arrows) were often solitary, but occasionally as in this case had multiple nodules apparently arising from distinct sites. Tumors frequently contained fluid-filled cavitory/pseudocystic structures (asterisks) that were filled with necrotic cellular debris. HE stain, bar = 730 μ m.

B) Tumors (arrows) compressed and effaced adjacent salivary gland tissue (asterisks). C) In some cases, tumor cells directly invaded (asterisk) gland interstitium, separating and effacing acini. HE stain, bar = B) 200 μ m and C) 100 μ m.

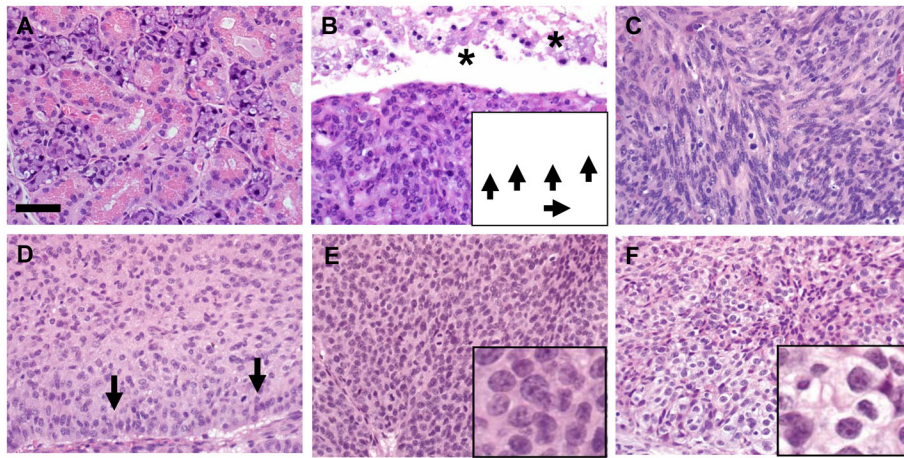


Figure 3. Histologic differentiation of salivary gland tumors

A) Normal appearance of WT submandibular salivary gland. B) Salivary gland tumors frequently contained cavitory/pseudocystic spaces (asterisks) filled by cellular debris and foamy macrophages. Tumor cells had frequent mitotic figures (arrows, inset). C) Tumor tissues commonly had interweaving cords of spindle cells. D) Tumors frequently contained sheets of epithelioid cells with palisading peripheral borders (arrows). E–F) Areas of basaloid (E) and clear cell (F) differentiation were observed (insets). HE stain, bar = 50 μ m.

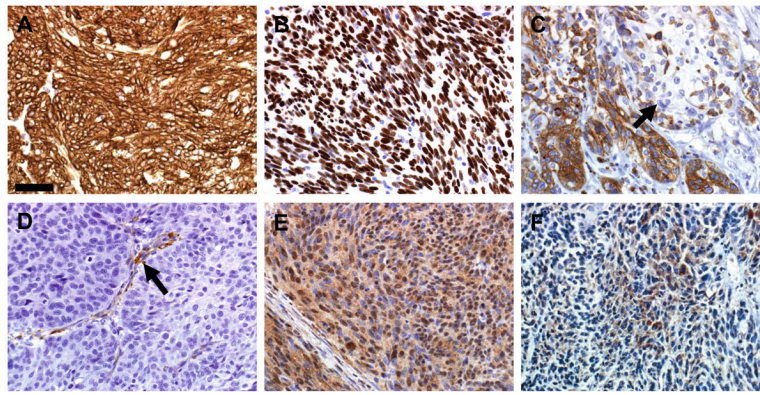


Figure 4. Immunohistochemical phenotyping of salivary gland tumors with cellular markers
A) Tumor cells had diffuse AE1/AE3 (pan cytokeratin) immunostaining. B) Tumor cells had widespread p63 nuclear immunostaining as compared to adjacent normal salivary gland (bottom) with only scattered myoepithelial nuclear immunostaining. C) Cytokeratin 5/6 immunostaining was present in well over 50% of tumor cells, but was often lacking in pleomorphic cellular foci (arrow). D) Tumor cells did not immunostain with *alpha*-smooth muscle actin, but the fibrovascular stroma (arrow) of the tumor did immunostain. E) EGFR immunostaining was widespread with mild to moderate intensity. F) pEGFR immunostaining was also detected in less extensive distribution than total EGFR (see Fig. 4E). Hematoxylin counter stain, bar = 50 μ m.

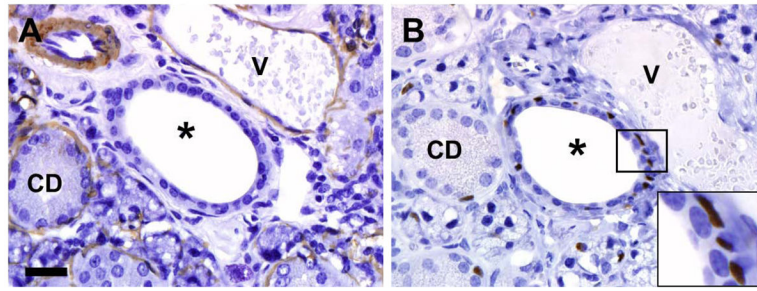


Figure 5. *alpha*-Smooth muscle actin (A) and p63 (B) immunostaining of *Justy* submandibular salivary gland

A) *alpha*-SMA immunostaining was present in myoepithelial cells surrounding epithelium of granular convoluted ducts (CD), vessels (V) and gland acini, but was absent in excretory ducts (*). B) p63 immunostaining was common seen subjacent to the excretory duct epithelium (see inset), but rarely detected around smaller convoluted ducts (CD). Hematoxylin counter stain, bar = 27 μ m.

Table 1

Primary antibodies and conditions for immunohistochemistry

| Marker | Source | Antibody Identifier | Dilution | Conditions |
|------------------|--------------------|----------------------------|-----------------|-------------------------------|
| AE1/AE3 | Novus Biologicals | Cat#NB600-1322 | 1:40 | HIER, citrate buffer (pH 6.0) |
| p63 | Neomarkers Company | Cat#MS-1081-P | 1:200 | HIER, citrate buffer (pH 6.0) |
| CK5/6 | Dako | Cat#M7237 | 1:100 | HIER, citrate buffer (pH 6.0) |
| EGFR | Abcam | Cat#ab2430 | 1:100 | HIER, citrate buffer (pH 6.0) |
| pEGFR | Abcam | Cat#ab40815 | 1:500 | HIER, citrate buffer (pH 6.0) |
| GFAP | Abcam | Cat#ab16997 | 1:100 | HIER, citrate buffer (pH 6.0) |
| cKIT | Dako | Cat#A4502 | 1:100 | HIER, citrate buffer (pH 6.0) |
| S100 | Dako | Cat#Z0311 | 1:4000 | HIER, citrate buffer (pH 6.0) |
| alpha-SMA | Sigma | Cat#A2547 | 1:2000 | None |

Table 2Clinicopathologic features of salivary gland tumors in *Justy* mice.

| Case | Age (months) | Proximal salivary glands | Histologic differentiation |
|------|--------------|---------------------------------------|--|
| 1 | 7 | Submandibular* | Spindled, epitheloid, basaloid, clear cell |
| 2 | 6 | Submandibular*, sublingual*, parotid* | Spindled, epitheloid, basaloid, clear cell |
| 3 | 8 | Submandibular* | Spindled, epitheloid |
| 4 | 10 | Submandibular* | Spindled, epitheloid, |
| 5 | 10 | Submandibular, sublingual, parotid | Spindled, epitheloid, basaloid |

*Tumor invaded interstitium and effaced salivary gland acini.

Author Manuscript

Author Manuscript

Author Manuscript

Author Manuscript

Table 3

Immunohistochemical markers and staining parameters

| Marker | Tumor Staining | Notes |
|------------------|-----------------|--|
| AE1/AE3 | +++ | Diffuse intense cytoplasmic staining of tumor cells; Adjacent normal gland had strong cytoplasmic staining of ducts and less intense staining of acini. |
| p63 | +++ | Diffuse nuclear staining in tumor cells; Adjacent normal gland had nuclear staining in periductular cells and in some cells between acini. |
| CK5/6 | ++ | Most tumors (>50%) had cytoplasmic staining that was more readily detected in the spindled tumor population than in the polygonal tumor cells; normal salivary gland had multifocal staining in periductal and less commonly periacinar stromal cells. |
| EGFR | ++ | Tumor cells showing patchy to coalescing staining; Adjacent gland had moderate staining in the ducts. |
| pEGFR | + / +++ | Tumor cells showing patchy to coalescing staining; Adjacent gland had weak multifocal staining in ducts |
| GFAP | Rare solitary + | Mostly negative with very rare solitary tumor cell immunostaining; Adjacent tissue had staining in nerves |
| cKIT | Neg | Tumor cells were negative; Ducts in adjacent glands had weak staining |
| S100 | Neg | Tumor was negative; Adjacent normal tissue had staining in peripheral nerves and moderate staining of salivary gland duct epithelium. |
| alpha-SMA | Neg | Negative in tumor cells. |

Scoring of tumor immunostaining: "Neg" - none; "+" rare to 33% of tumor cells; "++" ~34% to 66% of tumor cells; "+++" ~67% to diffuse cellular immunostaining